Available online at www.sciencedirect.com
ScienceDirect
Journal of the European Ceramic Society 28 (2008) 1763–1768
www.elsevier.com/locate/jeurceramsoc

# The role of magnesium on the stability of crystalline sepiolite structure

A. Esteban-Cubillo [a], R. Pina-Zapardiel [a], J.S. Moya [a,*], M.F. Barba [b], C. Pecharromán [a]

[a] *Instituto de Ciencia de Materiales de Madrid, CSIC, Cantoblanco, Madrid 28049, Spain*
[b] *Instituto de Cerámica y Vidrio, CSIC, Cantoblanco, Madrid 28049, Spain*

Received 22 August 2007; received in revised form 13 November 2007; accepted 16 November 2007
Available online 11 March 2008

**Abstract**

Sepiolite is a hydrate magnesium silicate special clay mineral. Some of the specific properties of this silicate are its large specific surface (about 320 $m^2/g$) together with a very reduced ion exchange capacity. Additionally, it is possible to leach the magnesium cations at the octahedral layer by acid attack, increasing the specific surface area up to the limit of the collapse of the structure. In the present investigation, we have found that the crystalline framework collapses when the fraction of leached $Mg^{2+}$ is greater than or equal to 0.33. Before the collapse it is possible to obtain sepiolite with different substituted metallic cations into the octahedral sites. As an example, the optimal composition of Ni–sepiolite was obtained after the lixiviation by acid attack at pH 0 for 1 h without the collapse of structure.


*Keywords:* Silicates; Sepiolite; Ion exchange; Crystal structure stability

## 1. Introduction

The peculiar structure of sepiolite ($Mg_8Si_{12}O_{30}(OH)_4(H_2O)_4{\cdot}8H_2O$) can be described as a quincunx arrangement of blocks separated by parallel channels[1] composed by two layers of $SiO_2$ tetrahedral enclosing a layer of MgO octahedral (Fig. 1). This structure induces needle-like particle shape, which contains open channels with dimensions of $3.6 \times 10.6$ Å running along the axis of the particle. Additionally, sepiolite has a large specific surface area (about 320 $m^2/g$) but a very reduced ion exchange capacity so that cations cannot be inserted inside the channels in ordinary clays or zeolites. Instead, they can be deposited on its surface by the addition of a basic solution.[2–4]

Conversely, it has been widely reported that in the activation process of the sepiolite by acid treatment,[5–9] the complete leach of the $Mg^{2+}$ cations takes place and then sepiolite transform into amorphous fibrous silica. However, the precise fraction of the leached $Mg^{2+}$ needed to collapse the original sepiolite structure and its influence in the further crystalline structure stability is still unknown.

In the present work, we have studied the changes produced in the sepiolite structure by means of acid treatments to increase the number of the acid centres at intracrystalline channels in order to generate enough octahedral vacancies before the full collapse of its structure. This knowledge opens the possibility to obtain sepiolite with different cations ($Ni^{2+}$, $Cu^{2+}$, $Fe^{2+}$, $Fe^{3+}$, ...) into the octahedral vacancies, which after the subsequent thermal reduction process, may become metallic nanoparticles embedded in a silicate matrix.[10,11] In this sense, $Ni^{2+}$ cations have been incorporated to the sepiolite silicate framework after different leaching treatments in order to check the stability of the sepiolite crystalline structure, and therefore the size, morphology and the stability of the corresponding metallic nanoparticles in sepiolite. In this regard, different techniques (X-ray diffraction (XRD), IR, transmission electron microscopy (TEM), Brunauer–Emmet–Teller (BET) and ICP) were used to characterize the resulting materials.

## 2. Experimental procedure

Natural sepiolite mineral from Vicalvaro-Vallecas (TOLSA, Spain) has been purified and micronized by a wet process to obtain a final product with higher than 95% content of sepiolite. The sepiolite needle-like particles have a length ranging from 0.2 to 2 μm and a thickness of 20–100 nm. Sepiolite powder was dispersed at 10 wt% concentration in water using high shear mixing. Then the suspension was acidified with HCl at pH 0 for different periods of time: 1–3, 6 and 24 h at a constant

* Corresponding author.
*E-mail address:* Jsmoya@icmm.csic.es (J.S. Moya).

0955-2219/$ – see front matter © 2008 Elsevier Ltd. All rights reserved.
doi:10.1016/j.jeurceramsoc.2007.11.022

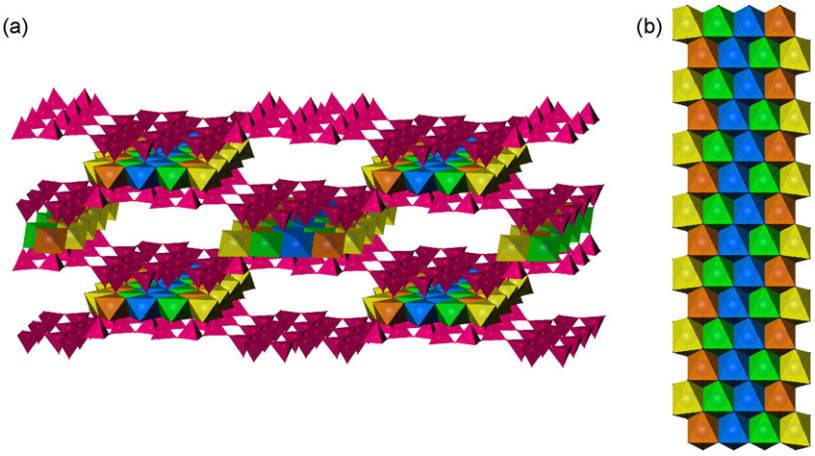


Fig. 1. (a) Crystallographic structure of the original sepiolite: silica tetrahedra in red, magnesium cations in different colours depending on their location in the octahedral layer. (b) Details of the magnesium octahedral layer from *c*-axis where distals appear in yellow, near to the edges in orange, near to the centre in green and in the centre edges of the magnesium layers in blue. (For interpretation of the references to color in this figure legend, the reader is referred to the web version of the article.)

temperature of 24 ± 1 °C. These samples were labelled as S1, S2, S3, S6 and S24, respectively, while S0 refers to the original sepiolite. The dispersions were vacuum filtered and washed with water.

On the other hand, sepiolite samples acidified at pH 0 for 1, 2 and 24 h were mixed with 1.0 l of aqueous solutions of $NiCl_2{\cdot}6H_2O$ salt. The concentration was adjusted so that the final metal content in sepiolite was 15 wt%. Thereafter, the pH of the dispersion was adjusted with NaOH to stabilize the suspension at pH 8.0. Finally, the dispersion was vacuum filtered and washed with water. The filtration cake was dried at 150 °C overnight, and then milled in an impact mill. The obtained precursors were reduced at 550 °C in a 10-vol.% $H_2$/Ar atmosphere to obtain nickel metallic nanoparticles laying inside the sepiolite particles.

X-ray diffraction patterns were recorded in a Bruker D8 diffractometer using Cu Kα radiation. Transmission electron microscopy images were taken by a JEOL microscope model FXII operating at 200 kV. Infrared spectroscopy was recorded in an IR Fourier transform Bruker IF66 V/S spectrophotometer. The fraction of the $Mg^{2+}$ cations leached was determined by inductively coupled plasma atomic emission spectrometry (ICP-OES), using a Thermo Jarrell Ash model Iris advantage spectrophotometer. The BET specific surface area of the different samples was determined using FlowSorb II 2300 equipment.

## 3. Results

In order to determine the maximum amount of $Mg^{2+}$ cations which can be removed from the sepiolite without modifying its crystalline structure, sepiolite suspensions have been treated at pH 0 for different periods of time. The XRD patterns corresponding to as received and treated sepiolite at pH 0 for 1, 2, 3, 6 and 24 h are shown in Fig. 2. In this plot it can be observed that samples treated for periods longer than 1 h, a band appears between 20° and 30° associated to amorphous silica. As a consequence, this band can be identified as a sign of sepiolite amorphization.

As well as the acid treatment modifies the crystallinity, it also changes the content and the coordination of the water molecules originally contained in the structure. In this sense, the study of the water vibration modes by IR spectroscopy (Fig. 3) can be a valuable tool to characterize the leaching process. Sepiolite IR spectra display bands at 3690, 3620, 3560, 3420, and 3256 $cm^{-1}$ corresponding to trioctahedral Mg–(OH), dioctahedral Mg–(OH), coordination water and zeolite water[12] modes, respectively. As it can be observed in Fig. 3b, these bands are very similar to the ones of the original sepiolite for sepiolite treated at pH 0 for 1 h but they broaden until they disappear for longer treatment time.[13,14]

The sepiolite bands at 1693, 1659 and 1623 $cm^{-1}$ correspond to stretching vibrations of water molecules.[15,16] After 1 h treatment at pH 0, the band at 1693 $cm^{-1}$ disappear while the rest of the bands are still visible (Fig. 3c). This missing band corresponds to coordinated water molecules which are bonded to $Mg^{2+}$ cations located at the edges of octahedral layer. After 2 h

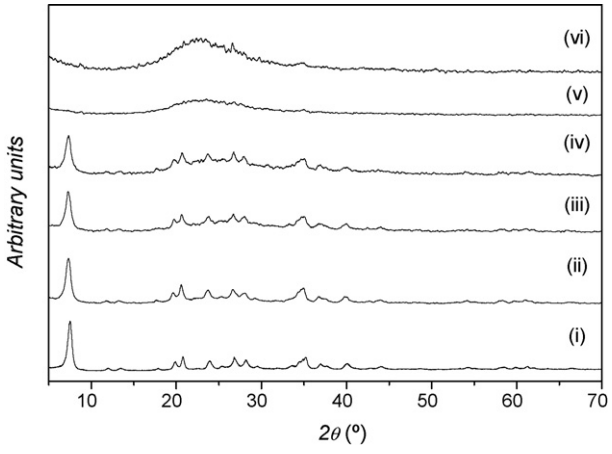


Fig. 2. XRD powder patterns corresponding to sepiolite (i), S1 (ii), S2 (iii), S3 (iv), S6 (v) and S24 samples (vi). S1, S2 and S3 samples display the diffraction peaks corresponding to sepiolite while XRD patterns of S6 and S24 samples are associated to amorphous silica.

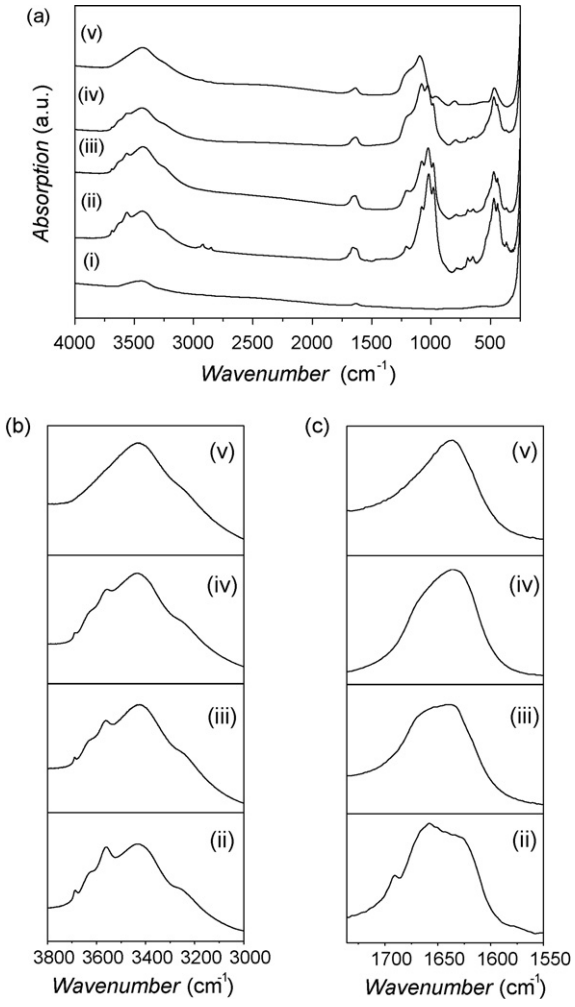


Fig. 3. (a) IR spectra of the KBr (i), S0 (ii), S1 (iii), S2 (iv) and S24 (v). Details of the bands display (b) between 3800 and 3000 $cm^{-1}$ and (c) between 1750 and 1560 $cm^{-1}$.

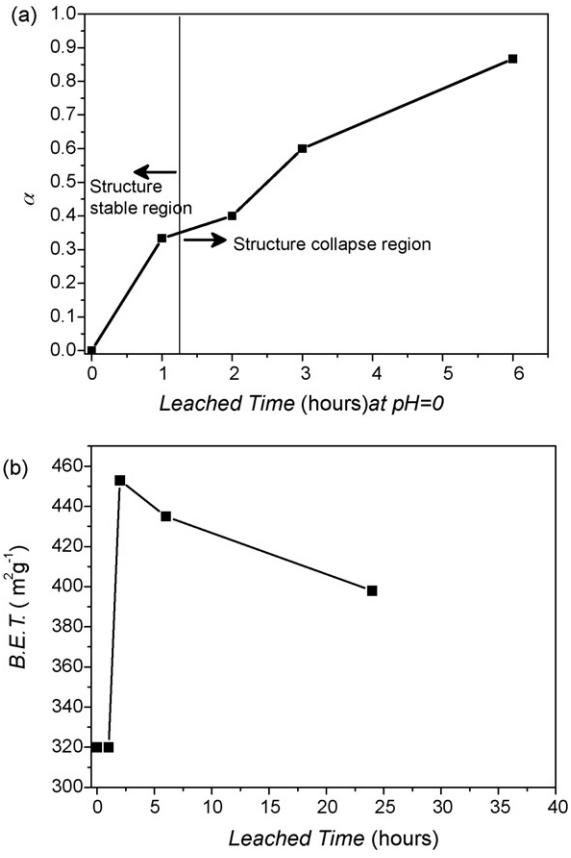


Fig. 4. (a) The $Mg^{2+}$ leaching evolution and (b) specific surface area of the sepiolite samples vs. leaching time.

of treatment the three modes cannot be distinguished to become, after a 24-h treatment, a single band located at 1637 $cm^{-1}$. This band can be assigned to bending vibrational mode of water. During the acid leaching, $Mg^{2+}$ cations are removed losing the water and hydroxyl group coordinated to them. This trend is similar to the one observed by XRD.

The bands at 1210, 1079, 1019 and 979 $cm^{-1}$ correspond to stretching vibrations of the Si–O bonds. These bands resulted to be very sensitive to the acid treatment. In fact, they broaden progressively for leaching time longer than 1 h. Additionally, as far as the samples loose their crystalline order, amorphous silica IR modes substitute those of sepiolite as it happens in S24 sample.[17,18]

In order to relate the crystalline stability with regards to the fraction of the $Mg^{2+}$ leached cations and to the specific surface area, we have analyzed the magnesium content of the samples acidified for different periods of time. Both the $Mg^{2+}$ cations leaching fraction ($\alpha$) and the specific surface area of the sepiolite samples versus treatment time are shown in Fig. 4. As it can be deduced from these plots, the sepiolite structure remains stable up to 1 h of acid treatment. According to ICP-OES chemical analyses (Fig. 4a), the maximum fraction of $Mg^{2+}$ leached at 1 h of treatment was found to be $\alpha = 0.33$ (5 wt% Mg). This leached fraction corresponds to the $Mg^{2+}$ cations located at edges of the octahedral layers and one $Mg^{2+}$ more per two unit cells (Fig. 1b). This $Mg^{2+}$ would be located next to the $Mg^{2+}$ cations into the distal position.

For higher leaching periods, crystalline structure collapses and therefore, a drastic increase of its specific surface area takes place. This is in good agreement with the presence of amorphous silica detected by XRD (Fig. 2) and the broadening of the bands in the corresponding IR spectra (Fig 3).

The morphology of the samples was studied by TEM. As can be observed in Fig. 5, the different sepiolite samples clearly point out that the morphology of the sample treated at pH 0 for 1 h does not show significant changes compared to the original sepiolite. However, after 2 h of acid treatment it has been found that a large fraction of sepiolite fibers break down (Fig. 5). The sample treated at pH 0 for 24 h, forms amorphous silica remaining its fibrous aspect, as it has been reported by previous works.[8,9]

## 4. Discussion

As it has been described in the introduction, it is well known that $Mg^{2+}$ cations can be leached from sepiolite structure by means of acid or acid and heating activation process to form

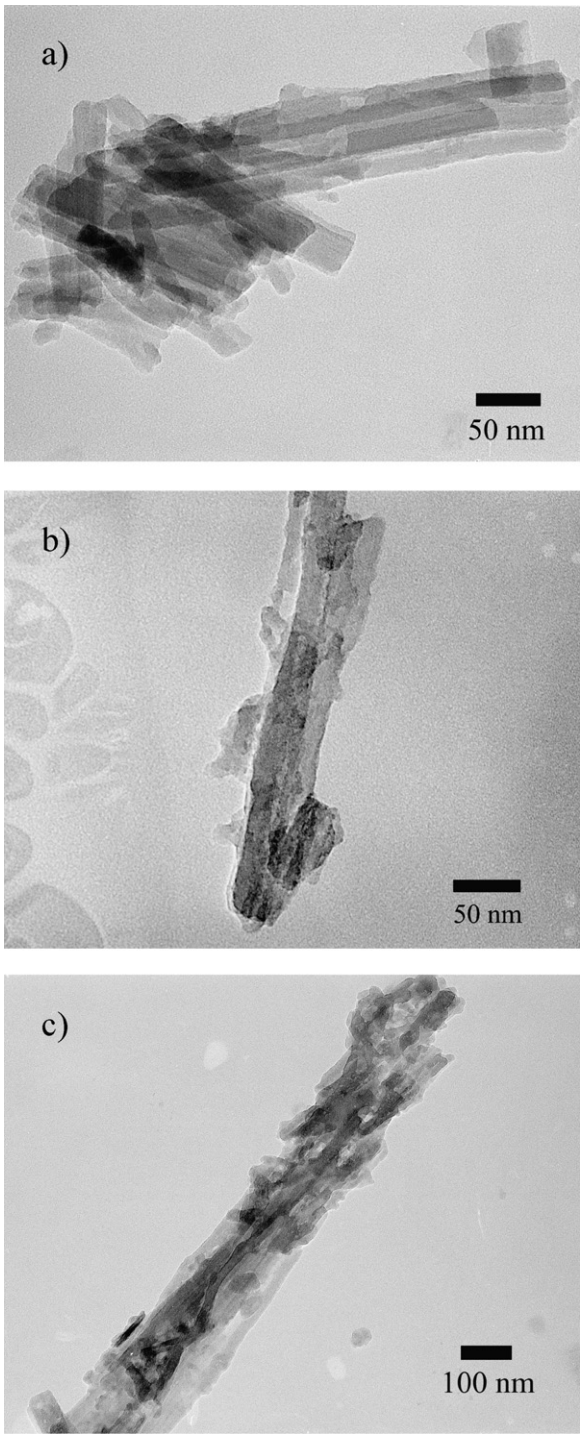


Fig. 5. TEM micrographs corresponding to (a) S1, (b) S2 and (c) S24 samples.

amorphous silica with a very large specific surface area. As a result of the collapse of its crystalline structure, fibers break down. On the contrary, in the present work, we are interested in finding out which is the critical specific fraction of $Mg^{2+}$ cations which can be leached before the collapse of the structure develops. In this sense, the magnesium layer leaching process generates a fraction of octahedral vacancies at the edges of the structural channels forming silanol groups[5,8,9] as follows:

$$Mg_8Si_{12}O_{30}(OH)_4(H_2O)_4\cdot 8H_2O + 2xH^+ \rightleftarrows Mg_{8-x}Si_{12-2x}O_{30-2x}(SiOH)_{2x}(OH)_4(H_2O)_4 \cdot 8H_2O + xMg^{2+}$$

Silanol groups act as Lewis acid centres. In agreement with the previous results (XRD, IR, and BET chemical analysis), it can be concluded that largest concentration of Lewis centres preserving the original sepiolite structure at room temperature ($24 \pm 1\,^{\circ}C$) is activated by an acid treatment at pH 0 for 1 h. This treatement leaches a relative $Mg^{2+}$ fraction of $\alpha = 0.33$ (5 wt% of the magnesium content on sepiolite) from the magnesium layer. Taking into account that sepiolite has four crystallographic sites[1] (Fig. 1), we propose that these leached $Mg^{2+}$ cations would correspond to 100% of the sites located at distal positions, and to approximately one-third of the $Mg^{2+}$ cations located at sites near the edges.[1]

This result means that sepiolite can be used as a host for different metallic cations. In fact, up to now, natural sepiolite was not employed for such purpose due to its very reduced ion exchange capability (C.E.C. 15 mequiv./100 g). Just for comparison, it should be reminded that in typical clays as montmorillonite,

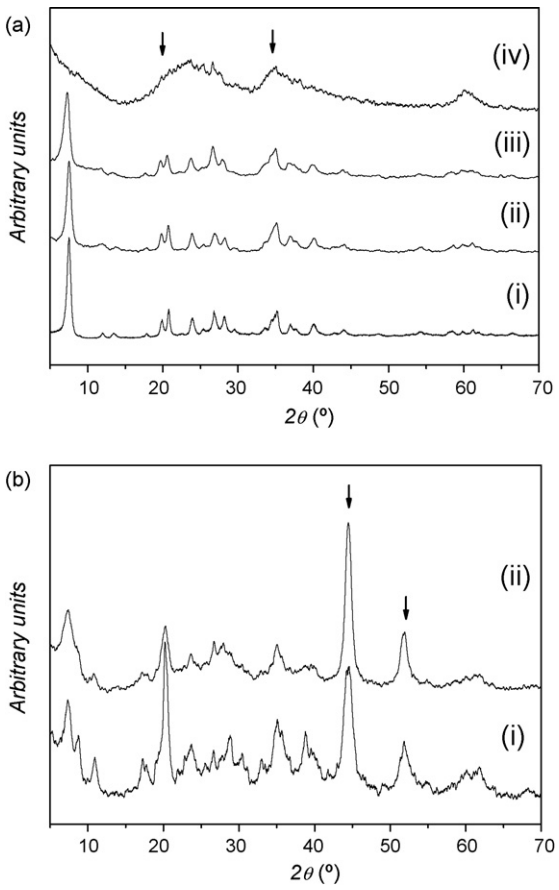


Fig. 6. XRD patterns corresponding to (a) sepiolite (i) and Ni–sepiolite treated at pH 0 for 1 h (ii), 2 h (iii) and 24 h (iv) (arrows show $Ni(OH)_2$ peaks); (b) Ni–sepiolite treated at pH 0 for 1 h (i) and 2 h (ii) reduced at 550 °C in $H_2$/Ar atmosphere (arrows show Ni peaks and the rest of peaks correspond to anhydrous sepiolite).

ion exchange capability is at least 10 times larger (C.E.C. 150 mequiv./100 g). However, a controlled leaching treatment is able to form enough silanol groups, distributed both on the surface and in the structural channels, to allow to incorporate a considerable amount of metallic cations (Cu, Ni, Fe, Co, Ag, Au, etc.) into the original octahedral positions.[10,19,20] In this regard, we have chosen the $Ni^{2+}$ cation because its water coordination sphere is very similar to that of $Mg^{2+}$ cations and $Ni^{2+}$ cations are more easily hydrolysed and consequently, it exhibits an adsorption pH lower than $Mg^{2+}$ cations:

$$Mg_{8-x}Si_{12-2x}O_{30-2x}(SiOH)_{2x}(OH)_4(H_2O)_4{\cdot}8H_2O + xNi^{2+} \rightleftarrows Mg_{8-x}Ni_xSi_{12}O_{30}(OH)_4(H_2O)_4{\cdot}8H_2O$$

The silanol groups generated during the acid activation at pH 0 for 1 h act as nucleation centres for the metal.[21] In this way, the final substitution of the leached $Mg^{2+}$ cations takes place during the addition of the NaOH solutions due to the amphoteric character of the silanol groups by uptaking the metal cations on these active sites[22–24]:

$$SiOH_2^+ \underset{+H^+}{\overset{-H^+}{\rightleftarrows}} SiOH \underset{+H^+}{\overset{-H^+}{\rightleftarrows}} SiO^- + H^+$$

That is, if the fraction of the leached $Mg^{2+}$ cations is $\alpha \leq 0.33$ the structure of the obtained Ni–sepiolite is identical to original sepiolite (Fig. 6a). Conversely, if the fraction of the leached $Mg^{2+}$ cations is $\alpha > 0.33$ (5 wt%), the sepiolite structure became damaged as it can be seen in Fig. 6a. The X-ray diffractogram shows a lost of crystallinity corresponding to some amount of amorphous silica present in the sample (Fig. 6a (iii)). In fact, when the sample is treated at pH 0 for 24 h, the sepiolite structure becomes completely amorphous and $Ni^{2+}$ cations cannot be incorporated into the sepiolite structure, so that they precipitate as $Ni(OH)_2$ at it can be observed in the XRD pattern (Fig. 6a). Therefore, although sepiolite particles maintains their fibrous aspect, its structural channels collapse avoiding the introduction of the metallic cations when the fraction of leached $Mg^{2+}$ cations is $\alpha > 0.33$ and then, these metallic cations are adsorbed as metallic hydroxides or oxyhydroxides on the silanols located at the fiber surface.

An appealing application of these metal substituted sepiolites consists in the possibility to obtain metallic nanoparticles. In this sense, Ni–sepiolite obtained under acid treatment at pH 0 for 1 and 2 h (Fig. 6b (i) and (ii), respectively) was reduced at 550 °C in $H_2$/Ar atmosphere. In both samples, peaks corresponding to metallic Ni were clearly observed. However, the samples treated at pH 0 for 1 h present a much minor particle size (<6 nm) than those treated at pH 0 for 2 h (15 nm), as observed by TEM (Fig. 7). It should be pointed out, that larger nickel particle sizes are obtained when $Ni^{2+}$ precipitated on the particle surface as $Ni(OH)_2$ nanoparticles, for samples corresponding to prolonged leaching treatments. However, if $Ni^{2+}$ cations incorporate into the sepiolite structure, the medium size of $Ni^{2+}$ clusters is much smaller. In this sense, after a reduction treatment it is possible to obtain Ni monodispersed nanoparticles completely covered and protected along the structural channels of the sepiolite, as can be observed in the TEM micrograph of Fig. 7.

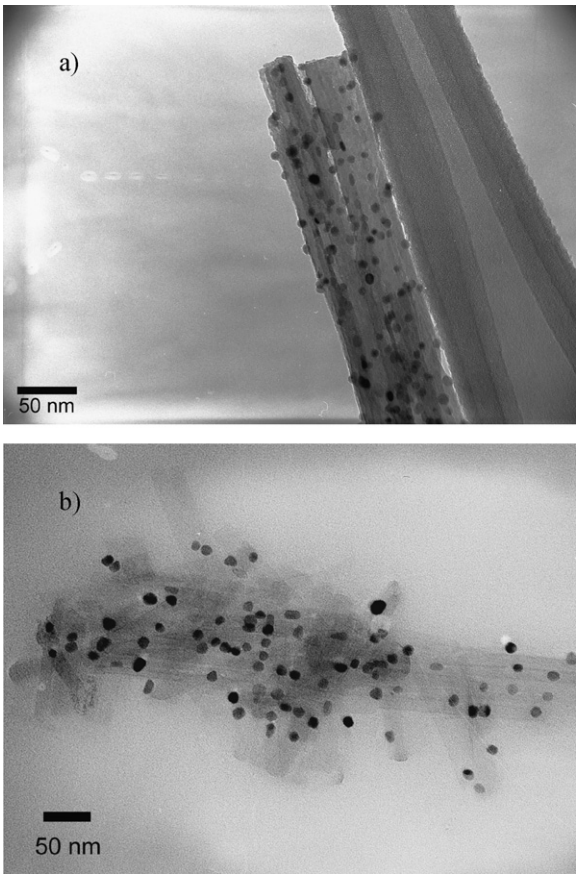


Fig. 7. TEM micrographs corresponding to (a) Ni–sepiolite treated at pH 0 for 1 h and (b) 2 h reduced at 550 °C in $H_2$/Ar atmosphere.

## 5. Conclusions

The limits of stability of the crystalline structure of the sepiolite versus the magnesium content have been studied. It has been found that when the fraction of $Mg^{2+}$ cations leached from the sepiolite ($\alpha$) is greater than or equal to 0.33, the sepiolite crystalline structure collapses forming amorphous silica. This fact opens the possibility to obtain sepiolite with different substituted cations along octahedral sites (metal–sepiolite). After a reduction process, it is possible to obtain metal monodispersed nanoparticles fully protected into the structural channels of the sepiolite as it has been proved in the case of the Ni–sepiolite.

## Acknowledgements

This work has been supported by the Spanish Ministry of Education and Science under projects MAT2006-10249-C02-01 and PTR1995-0832-OP in collaboration with TOLSA S.A. A.E.C. thanks to the financial support of the I3P grant by CSIC and European Social Fund (ESF).

## References

1. Brauner, K. and Preisinger, A., Structur und Enststehundg, TschermarksMineral. *Petrogr. Mitt.*, 1956, **6**, 120.

2. Esteban-Cubillo, A., Tulliani, J. M., Pecharromán, C. and Moya, J. S., Iron-oxide nanoparticles supported on sepiolite as a novel humidity sensor. *J. Eur. Ceram. Soc.*, 2007, **27**, 1983–1989.
3. Aramendia, M. A., Borau, V., Corredor, J. I., Jiménez, C., Marinas, J. M., Ruiz, J. R. *et al.*, Characterization of the structure and catalytic activity of Pt/sepiolite catalysts. *J. Colloid Interf. Sci.*, 2000, **227**, 469.
4. Corma, A., Mifsud, A., and Pérez Pariente, J., Procedimiento de Preparación de un Catalizador Metálico Soportado, Selectivo Para Procesos de Hidrogenación deshidrogenación. Patent ES-524261, 1983.
5. González, L., Ibarra, L. M., Rodríguez, A., Moya, J. S. and Valle, F. J., Fibrous silica gel obtained from sepiolite by HCl attack. *Clay Miner.*, 1984, **19**, 93–98.
6. Kara, M., Yuzer, H., Sabah, E. and Celik, M. S., Adsorption of cobalt from aqueous solutions onto sepiolite. *Water Res.*, 2003, **37**, 224–232.
7. Hernández, L. G., Rueda, L. I., Díaz, A. R. and Antón, C. C., Preparation of amorphous silica by acid dissolution of sepiolite: kinetic and textural study. *J. Colloid Interf. Sci.*, 1985, **1**(109), 150–160.
8. Jiménez-López, A., López-González, J. D., Ramírez-Sáez, A., Rodríguez-Reinoso, F., Valenzuela-Calahorro, C. and Zurita-Herrera, L., Evolution of surface area in a sepiolite as a function of acid and heat treatments. *Clay Miner.*, 1978, **13**, 375–385.
9. Sabah, E., Turan, M. and Celik, M. S., Adsorption mechanism of cationic surfactants onto acid- and heat-activated sepiolites. *Water Res.*, 2002, **36**, 3957–3964.
10. Pecharromán, C., Esteban-Cubillo, A., Montero, I. and Moya, J. S., Monodisperse and corrosion-resistant metallic nanoparticles embedded into sepiolite particles for optical and magnetic applications. *J. Am. Ceram. Soc.*, 2006, **89**(10), 3043–3049.
11. Esteban-Cubillo, A., Pecharromán, C., Aguilar, E., Santarén, J. and Moya, J. S., Antibacterial activity of copper monodispersed nanoparticles into sepiolite. *J. Mater. Sci.*, 2006, **41**, 5208–5212.
12. Frost, R. L. and Ding, Z., Controlled rate thermal analysis and differential scanning calorimetry of sepiolites and palygorskites. *Thermochim. Acta*, 2003, **397**, 119.
13. Ahlrichs, J. L., Serna, C. and Serratosa, J. M., Structural hydroxyls in sepiolites. *Clays Clay Miner.*, 1975, **23**, 119–124.
14. Vicente-Rodríguez, M. A., Suarez, M., Bañares-Muñoz, M. A. and Lopez-Gonzalez, J. D., Comparative FT-IR study of the removal of octahedral cations and structural modifications during acid treatment of several silicates. *Spectrochim. Acta Part A*, 1996, **52**, 1685–1694.
15. Corma, A., Pariente, J. P., Fornes, V. and Mifsud, A., Surface-acidity and catalytic activity of a modified sepiolite. *Clay Miner.*, 1984, **19**, 673–676.
16. Serna, C. J. and Vanscoyoc, G. E., Infrared study of sepiolite and palygorskite surface. In *Proceedings of the International Clay Conference*, ed. M. M. Mortland and V. C. Farmer. Elsevier, Amsterdam, 1978, pp. 197–206.
17. Akyuz, S. and Akyuz, T., FT-IR spectra of natural loughlinite (Na–sepiolite) and adsorption of pyrimidine on loughlinite. *J. Mol. Struct.*, 2004, **705**, 147–151.
18. Etchepare, J., Merian, M. and Kaplan, P., Vibrational normal modes of $SiO_2$. II. Cristobalite and tridymite. *Chem. Phys.*, 1978, **68**, 1531.
19. Corma, A., Pérez-Pariente, J. and Soria, J., Physico-chemical characterization of $Cu^{2+}$-exchanged sepiolite. *Clay Miner.*, 1985, **20**, 467.
20. Vico, L. I., Acid–base behaviour and $Cu^{2+}$ and $Zn^{2+}$ complexation properties of the sepiolite/water interface. *Chem. Geo.*, 2003, **198**, 213.
21. Lamer, V. K. and Dinegar, R. H., Theory, production and mechanism of formation of monodispersed hydrosols. *J. Am. Chem. Soc.*, 1950, **11**(72), 4847–4854.
22. Ersoy, B. and Celik, M. S., Electrokinetic properties of clinoptilolite with mono- and multivalent electrolytes. *Micropor. Mesopor. Mater.*, 2002, **55**, 305–312.
23. Doğan, M., Alkan, M. and Cakir, Ü., Electrokinetic properties of perlite. *J. Colloid Interf. Sci.*, 1997, **192**, 114–118.
24. Clause, O., Bonneviot, L., Che, M. and Dexpert, H., EXAFS characterization of the adsorbed state of Ni(II) ions in $Ni/SiO_2$ materials prepared by deposition–precipitation. *J. Catal.*, 1991, **130**, 21–28.